Available online at www.sciencedirect.com

SciVerse ScienceDirect

Ceramics International 38 (2012) 3735–3739

CERAMICS INTERNATIONAL

www.elsevier.com/locate/ceramint

Photovoltaic property dependence of dye-sensitized solar cells on sheet resistance of FTO substrate deposited via spray pyrolysis

Suk In Noh [a], Hyo-Jin Ahn [a,**], Doh-Hyung Riu [a,b,*]

[a] Department of Materials Science & Engineering, Seoul National University of Science and Technology, Seoul 139-743, Republic of Korea
[b] Research Institute for Solar Ceramic, SolarCeramic Co., Ltd., Seoul 153-801, Republic of Korea

Received 13 December 2011; received in revised form 9 January 2012; accepted 9 January 2012
Available online 16 January 2012

Abstract

F-doped SnO_2 (FTO) glass substrate was successfully fabricated via spray-pyrolysis deposition for use as a transparent conducting substrate in dye-sensitized solar cells (DSSCs). To investigate the performance dependence of DSSCs on the sheet resistance of the FTO films, three types of FTO films with sheet resistance values of 2 Ω/□, 4 Ω/□, and 10 Ω/□ were fabricated. Commercial FTO films having a sheet resistance of 15 Ω/□ were prepared for comparison. The structural, electrical, and optical properties of FTO films were characterized by scanning electron microscopy (SEM), atomic force microscopy (AFM), X-ray diffraction (XRD), X-ray photoelectron spectroscopy (XPS), the four-point probe method, and UV–vis spectrometry. The photocurrent–voltage data show that DSSCs fabricated with a sheet resistance of 2 Ω/□ exhibit the best photoconversion effciency (~5.5%) among the four samples. The performance improvement of DSSCs is due to improved short-circuit current density (~13.7 mA/cm^2) and fill factor (~62.3%).

Keywords: Films; Grain size; Electrical properties; Optical properties; Dye-sensitized solar cells; FTO

1. Introduction

Dye-sensitized solar cells (DSSCs), which are based on the principle of photosynthesis, have recently been received great attention in academic and industrial fields because of their advantages over conventional silicon photovoltaics, such as cost-effective fabrication, and attractive features, including transparency and flexibility [1,2]. In general, DSSCs consist of a nanoporous TiO_2 working electrode, electrolytes including a I^-/I_3^- redox couple, a platinum counter electrode, and a transparent conductive oxide (TCO) substrate [3]. The development of a suitable TCO substrate could be one of the most vital factors for improving the performance of DSSCs.

TCOs, which have high electrical conductivity and high optical transmittance, are doped metal oxide semiconductors with wide band gaps (~3 eV), such as SnO_2, In_2O_3, ZnO, CdO, and Ga_2O_3. It is well known that Sn-doped In_2O_3 (ITO), Al-doped ZnO (AZO), and F-doped SnO_2 (FTO) are now the most widely used TCO materials. In particular, FTO was widely used as a TCO substrate for DSSCs because of its stability at high temperatures and in acid atmospheres. So far, much effort has been devoted to the fabrication of a high-quality, high-performance FTO film using various synthetic methods, namely, sputtering, pulsed laser deposition, chemical vapour deposition (CVD), printing, and spray-pyrolysis deposition (SPD) [4]. Among the various synthetic methods, SPD has the advantages of being a simple, cost-effective, and scalable technique [5]. Several groups have demonstrated the electrical and optical properties of the FTO substrate fabricated by SPD. For example, Bisht et al. reported the comparison of FTO, ATO, and ITO coatings for flat and bent glass substrates synthesized via SPD together with their electrical and optical properties [6]. Ren et al. synthesized textured SnO_2:F thin films by SPD. They investigated important properties of the film structure, morphology, transmittance, and sheet resistance related to film temperature and thickness [7]. Arca et al. recently reported alternative fluorine precursors using benzenesulfonyl fluoride (BSF) for the fabrication of SnO_2:F thin films synthesized by SPD [8]. However, the performance dependence of DSSCs on

* Corresponding author.
** Co-corresponding author. Tel.: +82 2 970 6622; fax: +82 2 973 6657.
E-mail addresses: hjahn@seoultech.ac.kr (H.-J. Ahn), dhriu15@seoultech.ac.kr (D.-H. Riu).

0272-8842/$36.00
doi:10.1016/j.ceramint.2012.01.018

various sheet resistances of FTO substrates fabricated via SPD is not fully understood at present.

In this work, we fabricated three types of samples with different sheet resistances, that is, 2 Ω/□, 4 Ω/□, and 10 Ω/□, and demonstrated how the relationship between their photovoltaic properties and different sheet resistances affects DSSC performance. We employed a conventional FTO film (15 Ω/□, Pilkington) for the comparison and also characterized their photovoltaic properties in DSSCs.

2. Experimental

2.1. Experimental

We fabricated three types of FTO films, which had different sheet resistances, by SPD for use in DSSCs. The precursor solution was prepared by dissolving the mixture solution of tin chloride penta-hydrate ($SnCl_4 \cdot 5H_2O$, Daejung) and ammonium fluoride (NH_4F, Aldrich) in de-ionized (DI) water containing 5% ethyl alcohol. The precursor concentration of $SnCl_4 \cdot 5H_2O$ was 0.68 M. For the NH_4F, the mol ratio of F/Sn was 1.765. The FTO film was synthesized by spraying the FTO coating solution on a 10 cm × 10 cm PD glass substrate using an ultrasonic nebulizer (1.2 MHz). The glass substrate was fed into the spray zone on a belt for film deposition. The distance between the spray nozzle and the heated substrate was precisely controlled. By varying the speed of belt motion, the time to deposit the film was adjusted to get three types of FTO films with sheet resistances of 2 Ω/□, 4 Ω/□, and 10 Ω/□, (referred to as sample A, sample B, and sample C, respectively). Sheet resistance (Ω/□) was examined using the four-point probe method (FPP-200, Dasol Eng., Korea).

A TiO_2 paste was fabricated using a mixture consisting of TiO_2 (P25, Degussa), hydroxypropyl cellulose (HPC, M_w ~80,000, Aldrich), acetyl acetone (Aldrich), and DI water. Then, the FTO glasses (15 × 15 mm^2) were coated with the TiO_2 paste using a squeeze-printing technique. The TiO_2 printed FTO glasses were dried at 80 °C for 30 min in a convection oven. After the drying process, the FTO glass substrates with TiO_2 layers were sintered at 500 °C in air for 1 h. For the dye adsorption, a working electrode was immersed in 0.5 mM $Ru(dcbpy)_2(NCS)_2$ (N719, Solaronix) solution for 24 h at room temperature in a dark room.

In order to fabricate a counter electrode, we printed Pt catalysts by a squeeze-printing technique using platinum sol (Pt-catalyst T/SP, Solaronix). An iodine electrolyte based on

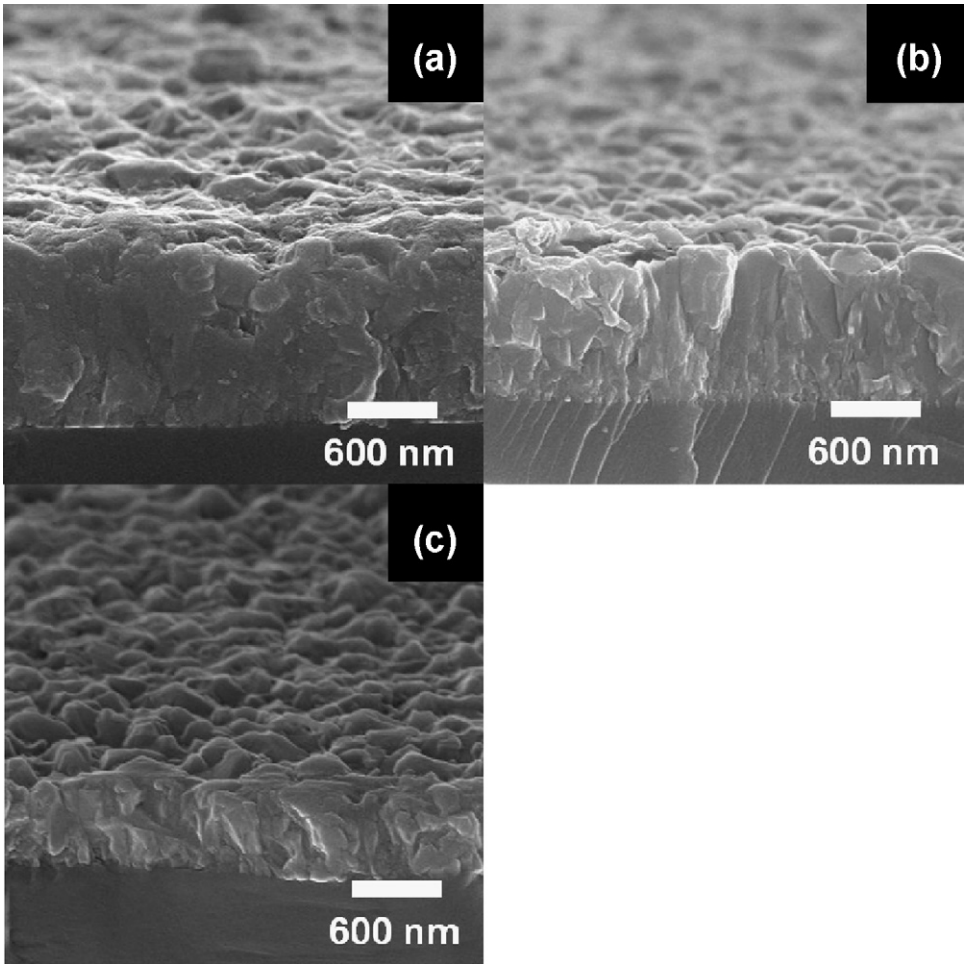

Fig. 1. Cross-sectional SEM images obtained from (a) sample A (2 Ω/□), (b) sample B (4 Ω/□), and (c) sample C (10 Ω/□) via SPD.

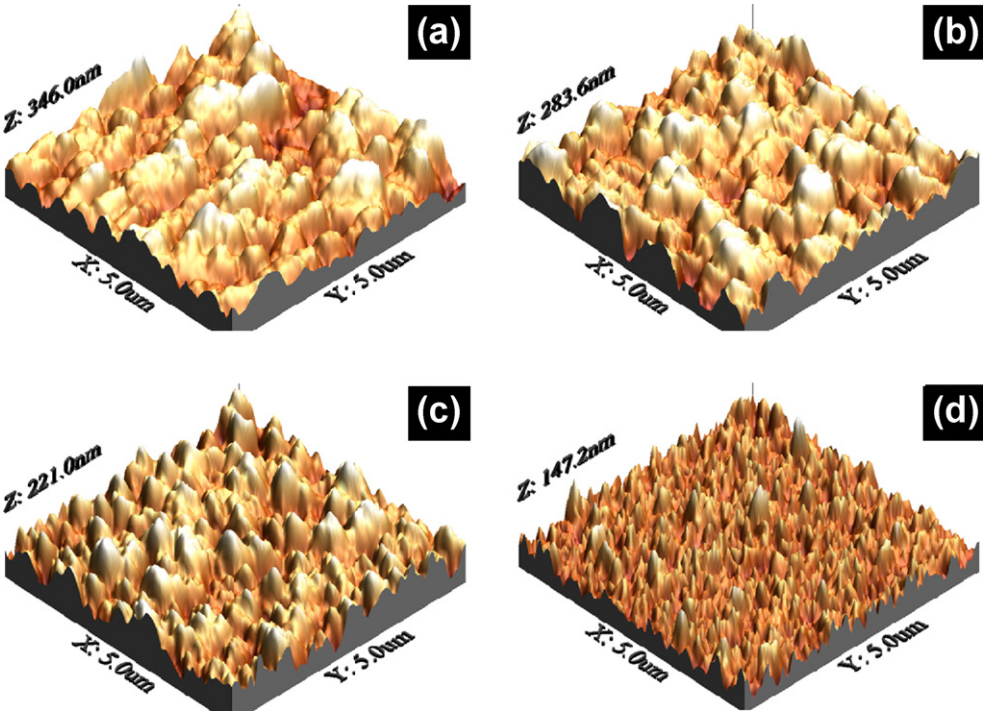

Fig. 2. 3-D AFM images of (a) sample A, (b) sample B, (c) sample C, and (d) the commercial FTO films.

0.3 M DMPII (Ionlic DMPII, Solaronix) was poured between the working and counter electrodes in the sandwich structure of the assembling cell.

2.2. Characterization

Cross sections of the FTO films were observed by field emission scanning electron microscopy (FE-SEM, Hitachi S-4700), and the morphologies of the FTO films were analyzed using an atomic force microscope (AFM, Albatross II). The crystallinity and chemical bonding states of the FTO films were characterized using X-ray diffraction (XRD, Rigaku Rint 2500 with Cu K_α radiation) and X-ray photoelectron spectroscopy (XPS, ESCA-LAB 250 with an Al Kα X-ray source). A UV–vis spectrophotometer (UV–vis, JASCO V650) was used in the wavelength range of 200 nm to 1100 nm to measure the optical transmission spectra of the FTO films. The photocurrent–voltage curves were examined using a 150 W xenon lamp (LAB 50) with a light intensity of 100 mA/cm^2 under standard irradiation (AM 1.5 Sun).

3. Results and discussion

Fig. 1 shows cross-sectional SEM images obtained from sample A (2 Ω/□), sample B (4 Ω/□), and sample C (10 Ω/□), which were fabricated via SPD. The film thicknesses were ∼1036–1296 nm for sample A, ∼920–1022 nm for sample B, and ∼511–627 nm for sample C. This implies that the thicker the FTO films, the lower their sheet resistance. Thus, sample A exhibits the thickest film and the lowest sheet resistance among the three types of FTO films. Furthermore, the sheet resistance of FTO films could be affected by the photovoltaic performance of DSSC devices, which will be discussed in detail in Fig. 6.

AFM analyses were carried out to examine the surface morphology of all the samples, as shown in Fig. 2. The surface morphology of FTO films affects their performance and hence that of the DSSCs. The average surface roughness was ∼43 nm for sample A, ∼38 nm for sample B, ∼29 nm for sample C, and ∼14 nm for the commercial FTO films. The AFM results indicate that the grain size gradually decreases from sample A to the commercial FTO films; that is, sample A shows the biggest grain size among all the samples. Results of the four-point probe method also indicate that sample A showed the lowest sheet resistance (2 Ω/□) among the three types of FTO films and the commercial FTO films; this may be because of the decrease in inter-grain boundaries caused by the bigger grain size, as shown in Fig. 2(a).

Fig. 3 shows the powder XRD patterns of samples A, B, and C, fabricated by SPD. In the case of all the samples, diffraction

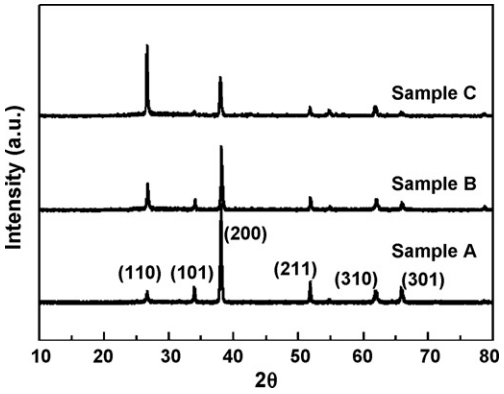

Fig. 3. Powder XRD patterns of sample A, sample B, and sample C fabricated by SPD.

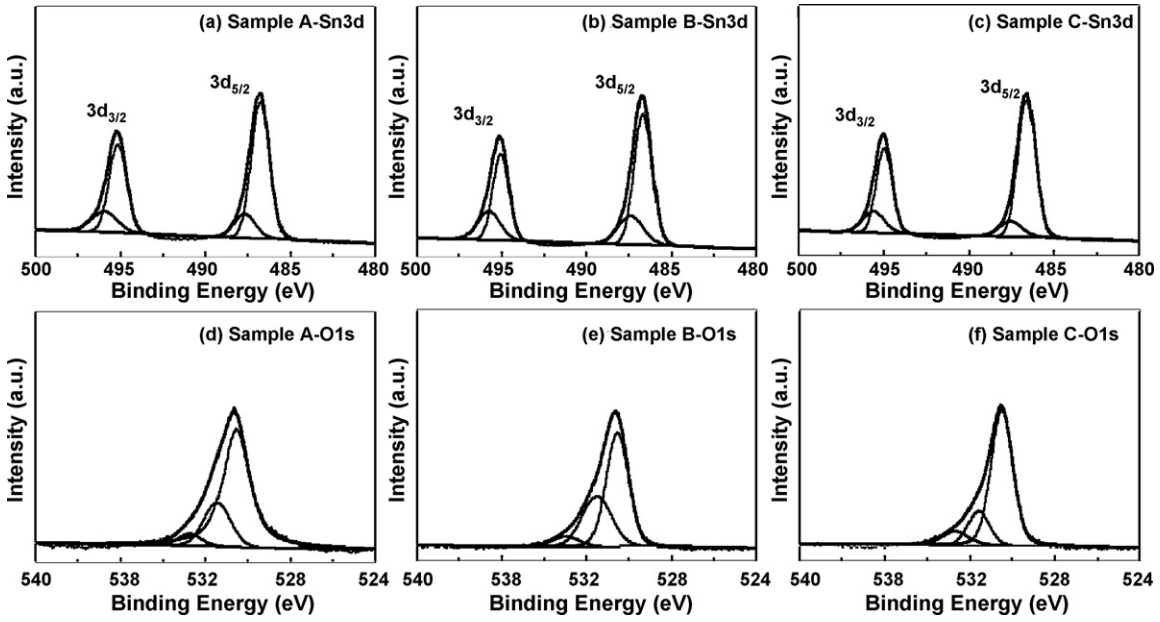

Fig. 4. (a)–(c) XPS spectra for the Sn $3d_{3/2}$ and $3d_{5/2}$ photoelectrons of sample A, sample B, and sample C at ~495.2 and ~486.8 eV. ((d)–(f)) XPS spectra for the O 1 *s* photoelectrons of sample A, sample B, and sample C at ~530.5 eV.

peaks were present at 26.6°, 33.8°, 37.9°, 51.7°, 61.8, and 65.9°, corresponding to the (1 1 0), (1 0 1), (2 0 0), (2 1 1), (3 1 0), and (3 0 1) planes. The observed sharp diffraction peaks show that all the samples had the cassiterite tetragonal (rutile type) structure (space group $p4_2/mnm$ (136)) (JCPDS card No.72-1147). The values of the lattice parameters, a lattice and c lattice, were calculated as ~4.74 Å and ~3.18 Å. These values agree with previously reported results [9,10]. As the thickness of FTO films increases, the strong diffraction peak relative to preferred-orientation moves from the (1 1 0) plane to the (2 0 0) plane, as shown in Fig. 3. As a result, the preferred orientation of FTO films is related to their resistivity and depends on the chemistry of the precursor solutions. When FTO films were grown from $SnCl_4$ solutions, the (2 0 0) preferred orientation was frequently reported. On the other hand, when FTO films were prepared using $SnCl_2$ solutions, a disordered preferential growth along (1 0 1), (2 1 1), and (3 0 1) has been reported [10]. Small amounts of alcohol added to the $SnCl_4$ water solution favoured the formation of the (2 0 0) preferred orientation films [11]. In this context, although the dependence of the electrical properties on the crystallographic preferred orientation is not yet clear, it is noted that FTO films having a strong diffraction peak relative to the (2 0 0) preferred orientation exhibited lower resistivity compared to the other preferred orientations, such as the (1 1 0) plane, which could cause a performance improvement in the DSSCs.

To further elucidate the elemental composition and chemical bonding states of the FTO films, XPS examinations were carried out on samples A, B, and C. Fig. 4 presents the XPS spectra of the Sn 3d and O 1s core level obtained from samples A, B, and C. The XPS spectra for the Sn $3d_{3/2}$ and $3d_{5/2}$ photoelectrons of samples A, B, and C were observed at ~495.2 and ~486.8 eV (Fig. 4(a)–(c)), implying that the elemental Sn in the SnO_2 is present as the Sn^{4+} species. In the case of Sn $3d_{5/2}$, the XPS spectra were composed of two peaks at ~487.7 eV and ~486.6 eV, corresponding to Sn–O bonding and Sn–F bonding states [9,12]. For the O 1s of samples A, B, and C (Fig. 4(d)–(f)), XPS spectra consisting of three different peaks were observed at ~530.5 eV for SnO_2, ~531.5 eV for C–O bonding states, and ~532.7 eV for $C–O_2$ bonding states. Thus, these results imply that the films fabricated by SPD are composed of SnO_2 with doped F.

Fig. 5 shows optical transmission spectra for samples A, B, C, and the commercial FTO films. The transmittances are observed to be ~46.2% for sample A, ~64.3% for sample B, ~67.1% for sample C, and 82.7% for commercial FTO films, respectively, at ~550 nm. These results show that the transmittance of the FTO films decreases with their thickness.

Fig. 6 shows photocurrent–voltage data of DSSCs fabricated with samples A, B, C, and the commercial FTO films. The short-circuit current densities (J_{sc}) for DSSCs fabricated with

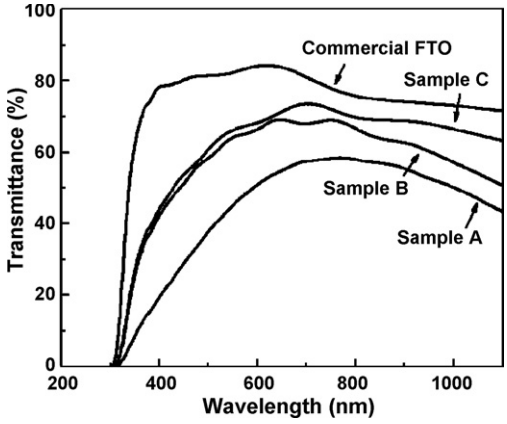

Fig. 5. Optical transmission spectra obtained from sample A, sample B, sample C, and the commercial FTO films.

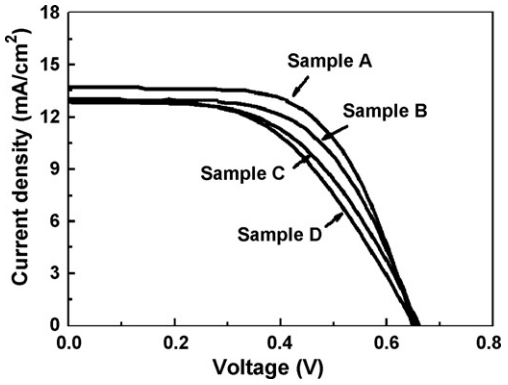

Fig. 6. Photocurrent–voltage data of DSSCs fabricated with sample A, sample B, sample C, and the commercial FTO films.

all the FTO films are ∼13.7 mA/cm^2 for sample A, ∼12.99 mA/cm^2 for sample B, ∼12.86 mA/cm^2 for sample C, and ∼12.91 mA/cm^2 for commercial FTO films. This implies that sample A, having the lowest sheet resistance, exhibits superior short-circuit current density compared to other samples. The open-circuit voltage (V_{oc}) for the samples exhibits almost same values of ∼0.66 V. The fill factors of all the samples are observed to be ∼62.3% for sample A, ∼59.0% for sample B, ∼53.8% for sample C, and ∼51.8% for the commercial FTO films. Interestingly, the lower the sheet resistance of the FTO film, the higher the fill factor of DSSCs. The photoconversion efficiency (η) of DSSCs fabricated with all the samples was calculated using the equation below [13]:

$$\eta(\%) = \frac{J_{sc} \times V_{oc} \times ff}{I_{max} \times V_{max}}$$

where J_{sc} is the short-circuit current density, V_{oc} is the open-circuit voltage, ff the fill factor, I_{max} the maximum power current, and V_{max} the maximum power voltage. The photoconversion efficiency (η) of all the samples is ∼5.52% for sample A, ∼5.02% for sample B, ∼4.58% for sample C, and ∼4.34% for the commercial FTO films. Thus, the photoconversion efficiency of sample A (2 Ω/□) is ∼27% higher than that of the commercial FTO films (15 Ω/□). This result implies that DSSCs fabricated with the FTO films having the lowest sheet resistance of 2 Ω/□ exhibit superior photoconversion efficiency compared to DSSCs fabricated with the FTO substrates having higher sheet resistances. The enhancement of photoconversion efficiency is explained in terms of the improved short-circuit current and the improved fill factor due to lower sheet resistance. Therefore, the use of FTO films with lower sheet resistance could improve the performance of DSSCs.

4. Conclusions

Three types of FTO films with different sheet resistances (2 Ω/□, 4 Ω/□, and 10 Ω/□) were fabricated by SPD. The dependence of the photovoltaic properties of DSSCs on the sheet resistance of FTO films was demonstrated. DSSCs fabricated with the FTO films having the lowest sheet resistance of 2 Ω/□ showed excellent short-circuit current density (∼13.7 mA/cm^2) and photoconversion efficiency (∼5.5%). DSSCs fabricated with FTO films having the lowest sheet resistance showed excellent photoconversion efficiency. These results indicate that the introduction of FTO films with the lowest sheet resistance could play a vital role in improving performance of high-efficiency DSSCs.

Acknowledgement

This research was supported by Basic Science Research Program through the National Research Foundation of Korea (NRF) funded by the Ministry of Education, Science and Technology (2011-0005561).

References

[1] E. Chadiri, N. Taghavinia, S.M. Zakeeruddin, M. Gratzel, J.E. Moser, Enhanced electron collection efficiency in dye-sensitized solar cells based on nanostructured TiO_2 hollow fibers, Nano Lett. 10 (2010) 1632–1638.
[2] M. Gratzel, Photoelectrochemical cells, Nature 414 (2001) 338–344.
[3] T. Soga, Nanostructured Materials for Solar Energy Conversion, Elsevier, 2006,, p. 193.
[4] J. Suffner, P. Agoston, J. Kling, H. Hahn, Chemical vapor synthesis of fluorine-doped SnO_2 (FTO) nanoparticles, J. Nanopart. Res. 12 (2010) 2579–2588.
[5] O. Vigil, L. Vaillant, F. Cruz, G. Santana, A. Morales-Acevedo, G. Contreras-Puente, Spray pyrolysis deposition of cadmium–zinc oxide thin films, Thin Solid Films 361–362 (2000) 53–55.
[6] H. Bisht, H.-T. Eun, A. Mehrtens, M.A. Aegerter, Comparision of spray pyrolyzed FTO, ATO and ITO coatings for flat and bent glass substrates, Thin Solid Films 351 (1999) 109–114.
[7] Y. Ren, G. Zhao, Y. Chen, Fabrication of textured SnO_2: F thin films by spray pyrolysis, Appl. Surf. Sci. 258 (2011) 914–918.
[8] E. Arca, K. Fleischer, I.V. Shvets, An alternative fluorine precursor for the synthesis of SnO_2:F by spray pyrolysis, Thin Solid Films 520 (2012) 1856–1861.
[9] W.Z. Samad, M.M. Salleh, A. Shafiee, M.A. Yarmo, Structural, optical and electrical properties of fluorine doped tin oxide thin films deposited using inkjet printing technique, Sains Malays. 40 (2011) 251–257.
[10] A. Smith, J.M. Laurant, D.S. Smith, J.P. Bonnet, R.R. Clemente, Relation between solution chemistry and morphology of SnO_2-based thin films deposited by a pyrosol process, Thin Solid Films 266 (1995) 20–30.
[11] C.Y. Kim, D.H. Riu, Texture control of fluorine-doped tin oxide thin film, Thin Solid Films 519 (2011) 3081–3085.
[12] J.F. Moulder, W.F. Stickle, P.E. Sobol, K.D. Bomben, Handbook of X-ray Photoelectron Spectroscopy, Physical Electronics, Physical Electronics, Inc., Eden Pairie, 1995, pp. 126–127.
[13] M. Gratzel, Dye-sensitized solar cells, J. Photochem. Photobiol. C 4 (2003) 145–153.